

# Landau Theory and the Emergence of Chirality in Viral Capsids

Sanjay Dharmavaram<sup>1</sup>, Fangming Xie<sup>4</sup>, William Klug<sup>1</sup>, Joseph Rudnick<sup>2</sup>, Robijn Bruinsma<sup>2,3\*</sup>

<sup>2</sup>*Department of Physics and Astronomy,*

<sup>1</sup>*Department of Mechanical and Aerospace Engineering,*

<sup>3</sup>*Department of Chemistry and Biochemistry, University of California, Los Angeles, CA 90095, USA and*

<sup>4</sup>*Department of Physics, University of Science and Technology of China, Hefei, Anhui, China*

We present a generalized Landau-Brazovskii theory for the solidification of chiral molecules on a spherical surface. With increasing sphere radius one encounters first intervals where robust achiral density modulations appear with icosahedral symmetry via first-order transitions. Next, one encounters intervals where fragile but stable icosahedral structures still can be constructed but *only* by superposition of multiple irreducible representations. Chiral icosahedral structures appear via continuous or very weakly first-order transitions. Outside these parameter intervals, icosahedral symmetry is broken along a three-fold axis or a five-fold axis. The predictions of the theory are compared with recent numerical simulations.

Landau theory is a central method for the analysis of phase transitions and spontaneous symmetry breaking. When complex fluids solidify, the emergent density modulations often adopt a variety of contending symmetries. Landau theory has been a powerful tool for the analysis of the phase diagrams [1]. In this letter, the Landau theory of the solidification of chiral molecules confined to a spherical surface is applied to the solidification of viral capsids [2, 3]. Capsids are spherical protein shells that surround viral genome molecules. Spherical viral capsids usually – though not always – have icosahedral symmetry [4]. On the other hand, numerical studies of systems of interacting particles confined to spherical surfaces find that icosahedral symmetry must contend with a variety of other symmetries [5],[6–9].

According to Landau theory, the density modulation of the ordered phase on a spherical surface should transform under the symmetry group  $G_0$  of the isotropic fluid phase according to a single irreducible representation (“irrep”) of  $G_0$ . The symmetry group  $G$  of the ordered phase must be an isotropy subgroup of  $G_0$ . Because the capsid proteins, or “subunits”, are chiral molecules (formed from the L-isomers of amino-acids)  $G_0$  should be the chiral group  $SO(3)$  of rotations without inversion. The density modulation of the ordered phase must then be expandable in the basis set of the  $2l + 1$  spherical harmonics  $Y_l^m$  for a particular  $l$  value, itself determined by minimization of the Landau free energy. As shown in refs. [10, 11], if one *demand*s that the ordered phase has chiral icosahedral symmetry, so with  $G$  the chiral icosahedral group  $I$ , then the expansion coefficients can be obtained from group theory. This leads to the icosahedral spherical harmonics  $\mathcal{Y}_h(l)$ [12]. Irreps of  $SO(3)$  with icosahedral symmetry can be constructed from even spherical harmonics for  $l = 6j + 10k$  with  $j, k \in \{0, 1, 2, \dots\}$  and from odd spherical harmonics for  $l = 15 + 6j + 10k$  [13]. If  $I$  is the isotropy subgroup then only odd values of  $l$  are allowed. This means that the smallest icosahedral capsids [4] should have surface density modulations proportional to  $\mathcal{Y}_h(l = 15)$  [10, 11] (maxima and minima of the density

modulation correspond here to the locations of subunits, whose density is odd under inversion).

The cubic non-linear term in the free energy density integrates to zero for odd  $l$ , which means that the solidification transition should be a *continuous transition*. This is surprising since solidification normally is a first-order transition [1]. This suppression of the first-order activation barrier by chirality would have important consequences for viral assembly. Models for protein-by-protein capsid assembly under equilibrium conditions encounter activation energy barriers that can be very large compared to the thermal energy [14]. If the solidification transition for chiral molecules on a spherical surface indeed has no activation barrier, then this could be an important argument in favor of collective descriptions of capsid assembly [2, 3, 15] as opposed to the protein-by-protein assembly models.

In this letter we re-examine the Landau theory for solidification on a spherical surface of molecules with chiral interactions [10, 11] now without requiring the density modulation to have icosahedral symmetry and without requiring it to be odd under inversion. Following other Landau theories of chiral complex liquids [16, 17], chirality is introduced here by including the lowest-order non-zero pseudo-scalar invariant of the order parameter in the free energy. The Landau-Brazovskii (LB) free energy density [1, 18] for solidification generalized to chiral systems is then

$$F = \int_{S^2} \left[ \left( \frac{1}{2} \left( (\Delta + k_0^2) \rho \right)^2 + \frac{r}{2} \rho^2 + \frac{u}{3} \rho^3 + \frac{v}{4} \rho^4 + \dots \right) + \chi \left( \nabla \rho \cdot (\nabla \nabla \rho)^2 \cdot (\mathbf{n} \times \nabla \rho) \right) \right] dS. \quad (1)$$

The integral is over a spherical surface  $S^2$ . The first term is the standard LB free energy density.  $\Delta$  is the Laplace-Beltrami operator on a spherical surface and  $k_0$  the ratio of the radius of the sphere and the characteristic length scale of the density modulation. Lengths are measured

in units of the sphere radius. The second part of the first term is an expansion of the free energy density in powers of the scalar invariants of the density modulation  $\rho$  with  $r$ ,  $u$ , and  $v$  the lowest-order expansion coefficients ( $u$  is negative and  $v$  is positive). The second term of Eq.1 is the lowest-order pseudo-scalar that can be constructed from  $\rho$  whose integral over a closed surface is non-zero [19]. Here,  $\mathbf{n}$  is a unit vector normal to the sphere surface and  $\chi$  is a parameter that measures the strength of chiral symmetry breaking [20].

Since the spherical harmonics  $Y_l^m$  are eigenfunctions of the  $\Delta$  operator with eigenvalue  $-l(l+1)$ , one can divide up the  $k_0$  axis into segments  $l^2 < k_0^2 < (l+1)^2$  so that in each segment the quadratic term in the free energy for that particular value of  $l$  first changes sign as one decreases the control parameter  $r$  [21]. The expansion coefficients of the density in the basis of  $Y_l^m$  are obtained by minimizing the full free energy, which results in  $2l+1$  coupled non-linear equations  $\langle Y_l^m | \frac{\partial F(\rho)}{\partial \rho} \rangle = 0$  [22]. For a particular solution of these equations to be stable, the eigenvalues of the Hessian matrix of second derivatives for that solution must be positive, apart from three eigenvalues that are zero associated with global rotation [23]. The first segment along the  $k_0$  axis that supports a non-trivial icosahedral subgroup is the one for  $l=6$ . The 13 coupled equations  $\langle Y_6^m | \frac{\partial F(\rho)}{\partial \rho} \rangle = 0$  are solved by  $\rho_6 = \xi \mathcal{Y}_h(6)$ . Here

$$\mathcal{Y}_h(6) = Y_6^0 + \sqrt{\frac{7}{11}}(Y_6^5 - Y_6^{-5}). \quad (2)$$

is the first non-trivial icosahedral spherical harmonic. The order parameter amplitude  $\xi$  obeys the cubic equation

$$r\xi + \tilde{u}\xi^2 + \tilde{w}\xi^3 = 0, \quad (3)$$

with  $\tilde{u} = u(50\sqrt{13}/323\sqrt{\pi})$  and  $\tilde{w} = 2145w/(1564\pi)$ . Equation 3 has the standard form of a first-order phase transition. The relevant eigenvalues of the  $13 \times 13$  Hessian matrix of the  $\rho_6$  solution branch are positive when the uniform state is unstable [24]. The coefficient  $\chi$  does not enter in Eq. 3 because the pseudoscalar invariant is zero in *any* of the  $2l+1$  dimensional subspaces [25]. Similar first-order solidification transitions to a stable icosahedral state take place in the subsequent  $l=10$  and  $l=12$  segments. If one identifies maxima of the density modulation with ‘‘capsomers’’ (groups of 5 or 6 subunits) rather than subunits themselves [7] then  $l=6$  corresponds to a  $T=1$  capsid and  $l=10$  and  $l=12$  to  $T=3$ , respectively,  $T=4$  capsids [26].

The next icosahedral intervals are for  $l=15, 16, 20$  and  $22$ . The icosahedral harmonics remain solutions of the projection equations  $\langle Y_l^m | \frac{\partial F(\rho)}{\partial \rho} \rangle = 0$  but their Hessian now has negative eigenvalues [27]. Stable icosahedral states that involve these icosahedral harmonics still can

be constructed but only by going beyond conventional Landau theory and include multiple irreps of  $\text{SO}(3)$ . As an example, in the enlarged product space of the  $l=15$  and  $l=16$  subspaces (denoted by ‘‘ $15 \times 16$ ’’) icosahedral density modulations would have the form

$$\rho(\zeta, \xi) = \zeta \mathcal{Y}_h(15) + \xi \mathcal{Y}_h(16), \quad (4)$$

The free energy has an extremum when the two-component order-parameter  $(\zeta, \xi)$  obeys a pair of coupled cubic equations [28]:

$$(c_{16}+r)\xi + u_1\xi^2 + u_2\xi^3 + v_1\xi^3 + v_2\xi^2 - \chi(3a_1\xi^2\zeta + a_2\zeta^3) = 0, \quad (5a)$$

$$(c_{15}+r)\zeta + u_3\xi\zeta + v_3\zeta^3 + v_4\xi\zeta^2 - \chi(a_1\xi^3 + 3a_2\zeta^2\xi) = 0, \quad (5b)$$

Numerical solution at the midpoint  $k_0 = 16$  between the  $l=15$  and  $l=16$  stability intervals shows that in that case the two components  $(\zeta, \xi)$  of the resulting order parameter are nearly proportional to each other and comparable in magnitude [29]. The chiral term in the free energy does not vanish in the enlarged  $15 \times 16$  subspace and now enters in these equations. For  $\chi = 0$ , there are two degenerate solutions, which we denote by D and L, that transform into each other under inversion (with  $\zeta \rightarrow -\zeta$ ). For  $\chi \neq 0$  but small, the free energy of the D and L branches shifts by an amount  $\Delta F_c = \chi(a_1\xi_0^3\zeta_0 + a_2\xi_0\zeta_0^3)$  where  $(\zeta_0, \xi_0)$  is the  $\chi = 0$  solution [30]. Since  $\Delta F_c$  is odd in  $\zeta_0$  the degeneracy between the D and L branches under inversion is lifted by an amount proportional to  $\chi$ . In the capsomer interpretation, the  $15 \times 16$  superposition state corresponds to the – intrinsically chiral –  $T=7$  shell while it correspond in the subunit interpretation to the  $T=1$  shell. In the latter case, the individual subunits are now neither odd nor even under inversion as is in fact the case for actual chiral molecules [31].

The stability of the superposition state is a sensitive function of the dimensionless radius  $k_0$ . Increasing the  $k_0$  parameter from the stability center of the  $l=15$  segment at  $k_0 \simeq 15.4$  towards the stability center of the  $l=16$  segment at  $k_0 \simeq 16.5$ , one finds that for decreasing  $r$  the uniform state initially does not transform directly into an icosahedral state. Instead, a stable superposition state appear only for values of  $r$  that are well below the stability limit of the uniform phase, as shown in Fig.1 A. Starting in this stable icosahedral state, and now increasing  $r$ , groups of three-fold degenerate eigenvalues  $\lambda_3 \propto (r - r^*(k_0))$  change sign at a first threshold  $r = r^*(k_0)$  (blue dot). Three corresponding eigenvectors of the Hessian with 2-fold, 3-fold, and 5-fold axial symmetry are shown in Fig.2. For  $r$  close to the stability limit of the uniform phase, one encounters a second instability point along the now unstable  $15 \times 16$  branch (red dot), where groups of four degenerate eigenvalues change

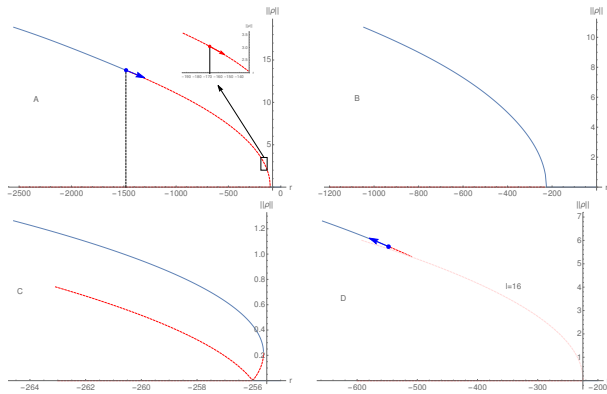


FIG. 1. Stability diagrams of the  $15 \times 16$  chiral icosahedral states for different values of the dimensionless radius  $k_0$ . Horizontal axis: control parameter  $r$ . Vertical axis: order parameter amplitude  $\|\rho\| = (\xi^2 + \zeta^2)^{1/2}$ . Solid blue: stable section. Dashed red: unstable section. (A):  $k_0 \simeq 15.8$  Blue dot: instability point of the icosahedral state against irrep 3. Red dot: instability points against irrep 4. (B):  $k_0 \simeq 15.9$ , (C):  $k_0 = 16$ , (D):  $k_0 \simeq 16.5$ . The unstable section is now mostly a pure  $l = 16$  state.

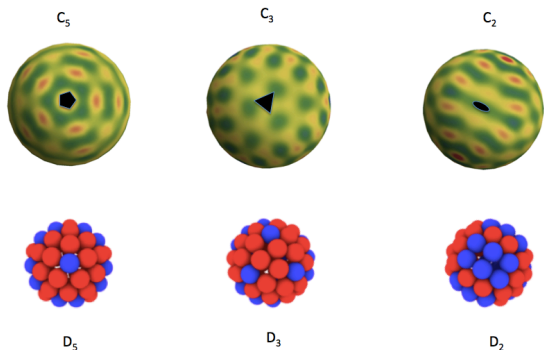


FIG. 2. (top) Three unstable eigenvectors of the Hessian of the  $15 \times 16$  chiral icosahedral states with, respectively,  $C_5$ ,  $C_3$ , and  $C_2$  rotational symmetry (left to right). (bottom) Competing groundstates of 72 one-state Lennard-Jones particles on a sphere with (left to right)  $D_5$ ,  $D_3$  and  $D_2$  symmetry. Blue spheres: 5-fold coordinated particles. Red spheres: 6-fold coordinated particles. From ref.[9] with permission.

sign. The corresponding eigenvectors have tetrahedral or  $D_3$  symmetry (see Fig.3). As  $k_0$  increases towards the boundary point  $k_0 = 16$ , both instability points slide down the stability curve and disappear around  $k_0 = 15.9$ . Over a short interval of  $k_0$  values, between 15.90 to 15.96 a stable  $15 \times 16$  branch appears directly from the uniform phase. Remarkably, within our numerical precision the transition indeed is continuous as shown in Fig.1 (B). For  $k_0$  slightly larger than 15.96. There still is a direct transition into the  $15 \times 16$  branch but the transition is now weakly first order (see Fig.1 C). As  $k_0$  increases

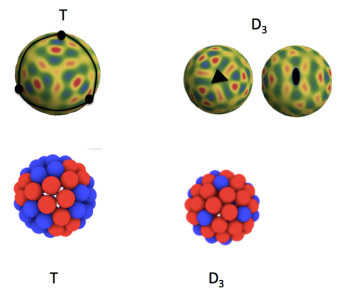


FIG. 3. (top) Unstable eigenvectors with tetrahedral and  $D_3$  symmetry. (bottom) Tetrahedral and  $D_3$  groundstates of 72 Lennard-Jones particles on a sphere. The two and three fold axes are perpendicular for  $D_3$ . From ref.[9] with permission.

towards the center of the  $l = 16$  stability segment at  $k_0 \simeq 16.5$ , the icosahedral state again becomes progressively less stable as shown in Fig.1 D [32].

The transition from the icosahedral state to one with lower symmetry can be analyzed by classical Landau theory. The symmetry group  $G_0$  is now the chiral icosahedral group  $I$ , which has one one-dimensional (“1D”) irrep, two 3D irreps, a 4D and a 5D irrep [33]. The first instability in Fig.1 (A) is associated with one of the two 3D irreps, denoted by 3, while the second is associated with the 4D irrep. The isotropy subgroups of  $I$  associated with the 3D irrep 3 are  $C_5$ ,  $C_3$ , and  $C_2$ . A natural orthogonal coordinate system in the 3D space of irrep 3 is one with the  $(1, 1, 1)$  direction along a three-fold symmetry direction, the  $(0, 0, 1)$  direction along a two-fold direction [34]. The order parameter is then a 3D vector  $\vec{\eta} = (\eta_1, \eta_2, \eta_3)$  in this space. Using symmetry arguments [35] the Landau energy  $\delta F(\vec{\eta})$  can be shown to have the form:

$$\delta F(\vec{\eta}) \propto \frac{\lambda_3}{2} |\eta|^2 + \frac{V}{4} |\eta|^4 + \frac{W}{6} |\eta|^6 + \Delta \frac{\sqrt{5}}{2} \eta_1^2 \eta_2^2 \eta_3^2 + \Delta \frac{\sqrt{5}}{60} (\eta_1^6 + \eta_2^6 + \eta_3^6) + \frac{\Delta}{4} (\eta_1^4 (\eta_3^2 - \eta_2^2) + \text{cyclic perm.}) \quad (6)$$

to sixth order in  $\eta$ . Here,  $\lambda_3$  is the eigenvalue that changes sign at the transition while  $V$  and  $W$  are positive constants [36]. A continuous transition takes place at  $\lambda_3 = 0$ . For  $\Delta = 0$ , the Landau energy is isotropic with arbitrary rotations in  $\vec{\eta}$  space connecting degenerate states. For  $\Delta$  negative, the minimum of  $\delta F(\vec{\eta})$  lies along the  $C_3$  direction and for  $\Delta$  positive along the  $C_5$  direction. For negative  $\lambda_3$ , the system thus has either a three-fold or a five-fold axis. The second instability in Fig.1 (top left) is associated with the 4D irrep, which has  $T$  and  $D_3$  as its isotropy subgroups. The corresponding eigenvectors are shown in Fig.3. The  $\delta F(\eta)$  for the 4D irrep contains cubic invariants in  $\eta$ . This means that icosahedral symmetry breaking in this case is discontinu-

ous. Finally, an instability driven by the 5D irrep would have  $D_2$ ,  $D_3$  and  $D_5$  as its isotropy subgroups.

Recently, numerical simulations of the groundstate of 72 “capsomer particles” on a spherical surface [7, 9] – corresponding to a  $T=7$  shell in the capsomer inter-creation – that interact via Lennard-Jones (LJ) interaction. Depending on parameters, they found an icosahedral groundstate as well as competing groundstates with  $D_2$ ,  $D_3$ ,  $D_5$ , and  $T$  symmetry (see Figs.2 and 3). They did not encounter however the  $C_3$  and  $C_5$  states. This suggests that for a LJ particle system, icosahedral symmetry is broken by the 4D and 5D irreps rather than the 3D irrep of LB theory.

What are the implications of these results for viral assembly? In the capsomer picture, a  $T = 1$  capsid appears via a robust first-order solidification transition and is quite stable. The capsid is chiral only in so far as capsomer particles are chiral. In the subunit picture, the  $T = 1$  capsid appears as a mixed  $15 \times 16$  state that is much less stable. It requires careful fine-tuning of the dimensionless radius  $k_0$ . The ordering transition of the subunit fluid is continuous or very weakly first-order. Chirality is now directly expressed in the subunit density modulation, which is neither even nor odd under inversion. There is apparently no unique Landau description and experiment may have to determine which one is appropriate. The  $T=7$  bacteriophage virus HK97 [37] may be an ideal “testbed” to test the theory. In the presence of high salt, Prohead 1 capsids of HK97 dissociate into interconverting pentamers and hexamers that are quite stable [38] so the capsomer picture is appropriate. The kinetics of Prohead 1 reassembly indicates that it is a highly cooperative process with some phase coexistence between capsids and capsomers [38], possibly consistent with the weakly first-order transition picture of Fig.1 B. Inducing point mutations on the genes for the capsid proteins could destabilize the fragile icosahedral state and reveal the instabilities of Fig.2. Next, the theory predicts that intrinsically chiral icosahedral capsids, such as  $T=7$  and  $T=13$ , should be very prone to undergo a transition into a lower symmetry state with  $C_3$  or  $C_5$  symmetry. The capsid should have an *oval deformation* for broken icosahedral symmetry because the corresponding eigenvectors are nearly odd under inversion. This has not yet been reported for HK 97 but capsids of the HIV virus do have an oval shape.

Finally, we note that the necessity of using of multiple irreps becomes less puzzling by noting that in the limit that the sphere radius goes to infinity, the density modulation should reduce to the superposition of three periodic density waves whose wavevectors make an angle of 120 degrees with respect to each other (a hexagonal crystal). The expansion of a plane wave into spherical harmonics requires an infinite series of  $l$  terms so an *infinite series of irreps* of  $SO(3)$  would be required to describe solidification in the limit of large sphere radii.

## ACKNOWLEDGMENTS

We would like to thank Vladimir Lorman and Alexander Grosberg for helpful discussions, the NSF for support under DMR Grant No. 1006128 and the Aspen Center for Physics for hosting a workshop on the physics of viral assembly.

---

\* sanjaydm@ucla.edu

- [1] E. Kats, V. Lebedev, and A. Muratov, Physics Reports **228**, 1 (1983).
- [2] R. Garmann, M. Comas-Garcia, A. Gopal, C. Knobler, and W. Gelbart, J. Mol. Biol. **426**, 1050 (2013).
- [3] R. F. Bruinsma, M. Comas-Garcia, R. F. Garmann, and A. Y. Grosberg, Phys. Rev. E **93**, 032405 (2016).
- [4] D. L. Caspar and A. Klug, in *Cold Spring Harbor symposia on quantitative biology*, Vol. 27 (Cold Spring Harbor Laboratory Press, 1962) pp. 1–24.
- [5] J. M. Voogd, PhD thesis, Universiteit van Amsterdam, 1994.
- [6] S. Fejer, D. Chakrabarti, and D. Wales, ACS Nano **4**, 219 (1988).
- [7] R. Zandi, D. Reguera, R. Bruinsma, W. Gelbart, and J. Rudnick, Proc Natl Acad Sci U S A. **101**, 15556 (2004).
- [8] H. Kusumaatmaja and D.J Wales, Phys. Rev. Lett. **110**, 165502 (2013).
- [9] S. Paquay, H. Kusumaatmaja, D. Wales, R. Zandi, and P. van der Schoot, <http://arxiv.org/abs/1602.07945> [cond-mat.soft] (2016).
- [10] V.L. Lorman and S.B Rochal, Physical Review B **77**, 224109 (2008).
- [11] V.L. Lorman and S.B. Rochal, Physical review letters **98**, 185502 (2007).
- [12] F. Klein, *Lectures on the Icosahedron and the Solution of the Fifth Degree* (Dover, 2003).
- [13] M. Golubitsky, I. Stewart, et al., *Singularities and groups in bifurcation theory*, Vol. 2 (Springer Science & Business Media, 2012).
- [14] R. Zandi, P. van der Schoot, D. Reguera, W. Kegel, and H. Reiss, Biophys. J. **90**, 1939 (2006).
- [15] O. Elrad and M. Hagan, Physical Biology **7**, 045003 (2010).
- [16] P. de Gennes and J. Prost, *Physics of Liquid Crystals* (Oxford, 1993).
- [17] W. Helfrich and J. Prost, Phys. Rev. A. **38**, 3065 (1988).
- [18] S. Brazovskii, Zh. Eksp. Teor. Fiz **68**, 175 (1975).
- [19] This term, which is similar to the chiral term of the Helfrich-Prost theory for curved chiral surfaces [17], is further discussed in section S1 of supplementary material.
- [20] To show that the uniform phase of this free energy has  $SO(3)$  symmetry rather than  $O(3)$  it is necessary to compute higher order density correlation function in the presence of thermal fluctuations.
- [21] The stability threshold is  $r_l(k_0) = -(k_0^2 - l(l+1))^2$ .
- [22] The explicit form of the equations is provided in section S2 of supplementary material.
- [23] Hessian matrices were diagonalized numerically using Mathematica.

- [24] See last paragraph of section S2 of supplementary material.
- [25] See section S3 of supplementary material.
- [26] The corresponding density modulations are shown in section S4 of the supplementary material.
- [27] It is shown analytically in section S5 of supplementary material that  $\mathcal{Y}_h(15)$  is unstable for any value of  $u$  and  $v$ .
- [28]  $c_{16} = (k_0^2 - 16 \times 17)^2$ ,  $c_{15} = (k_0^2 - 15 \times 16)^2$ ,  $a_1/16 = -80.4$ ,  $a_2/16 = -3084.1$ ,  $u_1 = 0.13494u$ ,  $u_2 = 0.234946u$ ,  $v_1 = 1.04204w$ ,  $v_2 = 0.681228w$ ,  $u_3 = 0.623577u$ ,  $v_3 = 0.789107w$ , and  $v_4 = 0.904033w$ .
- [29] The resulting density modulations are shown in section S6 of the supplementary material and compared with the result of a two-state MC simulation of T=7 CK capsids composed of 72 capsomers [7].
- [30] There is also a shift of the two branches by a term that is even in  $\zeta$ .
- [31] This is illustrated in Fig. S4 of the supplementary material section S6. Similar results hold for larger values of  $l$ . For example, the  $21 \times 22$  branch produces a chiral T=3 shell in the subunit picture and a T=13 shell in the capsomer picture. The  $20 \times 21$  branch produces a chiral T=2 non-CK icosahedral shell.
- [32] The instability sequence is not symmetric around  $k_0 = 16$ : the unstable icosahedral branch now mostly is a pure  $l = 16$  icosahedral harmonic with the  $15 \times 16$  state only appearing close to the stability limit of the icosahedral state.
- [33] R. Hoyle, *Physica D* **191**, 261 (2004).
- [34] The direction  $\eta_1 = 0$  and  $\eta_2^2 = 1/2(3 - 5^{1/2})\eta_3^2$  is then along a 5-fold axis.
- [35] See section S7 of Supplementary Material supplementary material.
- [36] The terms proportional to  $W$  and  $\Delta$  in Eq.6 are generated by sixth and higher order terms in  $\rho$  in the LB free energy density Eq. 1.
- [37] J. Conway, W. Wikoff, N. Cheng, R. Duda, R. Hendrix, J. Johnson, and A. Steven, *Science* **292**, 744 (2001).
- [38] Z. Xie and R. Hendrix, *J. Mol. Biol.* **253**, 74 (1995).